Table 2 Mean Distance from the Probes to the Poly(A) Tail Positions of Genes Showing Presence Solely in the UFT or Methacarn-Fixed PET[a]

aRNA Sample	UFT, 1× amplified	Methacarn-Fixed PET, 2× amplified
Mean distance from the 5′ end of the poly(A) tail (bp)		
No. of genes examined[b]	6	5
3′ end of the 5′ most probe	847	318[c]
3′ end of the 3′ most probe	569	97[c]

aRNA, antisense RNA; UFT, unfixed frozen tissue; PET, paraffin-embedded tissue.

[a] Genes obtained from microarray data in Table 1 were examined.

[b] All genes with sequence information for the 3′-untranslated region were examined.

[c] Significantly different from the unfixed frozen samples ($p < 0.01$).

ferences for male- or female-biased expression were found for 21% and 6% of all present genes, respectively (≥2-fold; Table 3). On EB-treatment, females demonstrated a greater number of genes with expression change. In males, up-regulation by EB was found for only 25 genes, all of them within 2- to 5-fold, and no genes showed down-regulation. In females, up-regulation was detected for a total of 586 genes after EB-treatment (≥2-fold), with 52 genes exhibiting ≥5-fold increase. When compared with up-regulated genes, down-regulated examples were fewer in number in females, with a total of 187 genes showing ≤1/2-fold down-regulation when compared with the vehicle control level. Among them, 33 genes showed ≤1/5-fold down-regulation when compared with vehicle controls. Relatively small numbers of genes showed altered expression on FA-treatment in both sexes. In males, only two and three genes showed up- and down-regulation, respectively (2- to 5-fold change), and in females, three and 22, all of them exhibiting 2- to 5-fold change, except for one gene with ≤1/5-fold up- and down-regulation, respectively.

Among genes showing male-biased expression (≥2-fold difference; 740 genes in total), 59% of them exhibited up-regulation on EB-treatment in females (≥2-fold; 437 genes in total), one of them also exhibiting up-regulation by FA in males (as shown in Fig. 4). One example alone showed down-regulation by FA in males. On the other hand, among genes showing female-biased expression (≥2-fold difference; 203 genes in total), 55% of them exhibited down-regulation by EB in females (≤1/2-fold; 111 genes in total). Among them, a total of 10 genes also showed altered expression by FA; nine genes down-regulated in females and one gene up-regulated in males. On the other hand, five female-predominant genes exhibited up-regulation by EB in males, four of them also showing down-regulation by EB in females, with one gene each further showing down-regulation in females and up-regulation in males by FA-treatment.

When genes that demonstrated changed expression levels in both sexes by the chemical treatments were examined, four genes encoding the LINE retrotransposable element 3, L1Rn B6 repetitive DNA element, ADP-ribosyltransferase (adprt) 1, and NonO/p54nrb homolog, exhibited up-regulation in males and down-regulation in females by EB-treatment and also female-biased expression (Table 4). Expression levels for genes showing male-biased expression were not affected by EB. FA-treatment did not alter the expression level of any gene involving both sexes.

Table 5 shows the list of genes showing altered expression in the MPOA of either sex common to both chemicals. Among the total of 15, 12 showed down-regulation in females common to EB and FA, eight of them exhibiting female-biased expression, i.e., for protein tyrosine phosphatase, receptor type, F (*PTPRF*); DAP-like kinase (*dlk*); glutamate receptor, kainate receptor subunit (KA1); dyskeratosis congenita 1 (*dyskerin*); L1Rn B6 repetitive DNA element; *MAP2*; expressed sequence tag (EST), similar to the mouse estrogen-responsive finger protein (*efp*); and glutamate receptor, ionotropic, AMPA subtype (GluR1).

Table 3 Number of Genes Showing Sex Differences in Basal Expression as well as Alteration After EB or FA Treatment in the Neonatal MPOA ($p < 0.05$)

Difference/Change (× fold)	2–5	≥5
Sex difference		
Males > females	676	64
Females > males	176	27
Altered by EB		
Males		
Up-regulated	25	0
Down-regulated	0	0
Females		
Up-regulated	534	52
Down-regulated	154	33
Altered by FA		
Males		
Up-regulated	2	0
Down-regulated	3	0
Females		
Up-regulated	3	0
Down-regulated	22	0

EB, estradiol benzoate; FA, flutamide; MPOA, medial preoptic area.

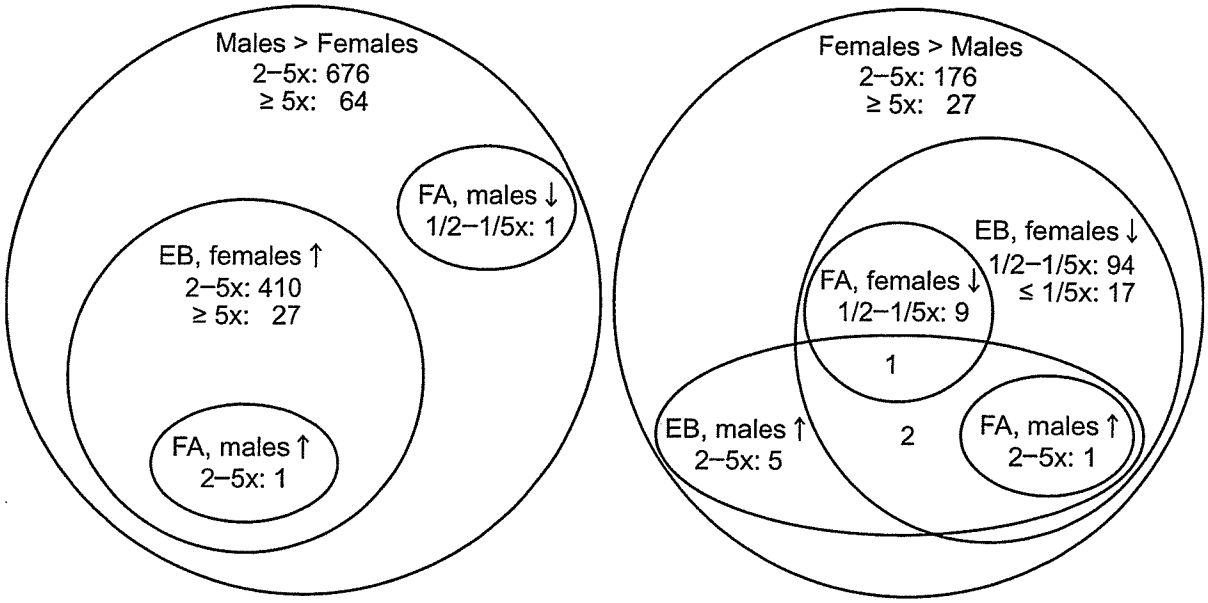

Figure 4 Distribution of gene populations showing altered expression with EB and/or FA-treatment among those showing sex differences in expression in the neonatal MPOA.

Interestingly, two subtypes of glutamate receptors, KA1 and GluR1, exhibited this particular expression pattern, the former being detected with two different probe sets (accession nos. U08257 and X59996). Without showing sex differences in the basal expression, expression of five genes were influenced by EB and FA, the following four exhibiting down-regulation in females with both chemicals: myeloid/lymphoid or mixed-lineage leukemia (trithorax (drosophila) homolog); translocated to, 3; cyclin D1; serine/threonine kinase 25; and neurotrimin. On the other hand, one EST (accession no. AI639097) showed up-regulation by EB and down-regulation by FA in females. Among the genes listed in Table 5, up-regulated examples were rather few and the magnitude of up-regulation was within 2- to 3-fold. In addition to the altered expression involving both sexes after EB treatment (see above), two genes showed altered expression with FA, i.e., down-regulation of the L1Rn B6 repetitive DNA element in females, and up-regulation of the LINE retrotransposable element 3 in males. Among those showing male-biased expression, there was only one with altered expression due to both EB and FA. MT1a transcripts showed up-regulation by EB in females and also by FA in males.

Fig. 5 shows mRNA expression data for two genes by real-time RT-PCR regarding sex differences in the neonatal MPOAs observed with microarrays. Both thymosin $\beta 4$ and $G\alpha i2$ mRNAs exhibited strong male-biased expression at PND 2, with 8.9- and 7.1-fold higher levels than in females. Real-time RT-PCR results confirmed this sex difference.

Immunoreactivity of Protein Signals

Fig. 6 shows representative figures for immunohistochemical demonstration of protein signals in the MPOA with the anatomical location indicated in

Table 4 List of Genes Showing Altered Expression in the MPOA of Both Sexes by EB-Treatment (≥2-fold, $p < 0.05$)

			Altered by EB (× fold *vs.* control)	
Accession No.	Gene	Sex Difference (× fold)	M	F
M13100	LINE retrotransposable element 3	M<F (2.9)	2.1	0.5
X07686	L1Rn B6 repetitive DNA element	M<F (3.8)	2.0	0.4
AA964849	ADP-ribosyltransferase (adprt) 1	M<F (3.3)	2.2	0.3
AF036335	NonO/p54nrb homolog	M<F (5.5)	3.2	<0.1

MPOA, medial preoptic area; EB, estradiol benzoate; FA, flutamide; M, males; F, females; EST, expressed sequence tag.

Table 5 List of Genes Showing Altered Expression in the MPOA Common to EB and FA (≥2-fold, $p < 0.05$)

Accession No.	Gene	Sex Difference (× fold)	Altered by EB (× fold *vs.* control)		Altered by FA (× fold *vs.* control)	
			M	F	M	F
M13100	LINE retrotransposable element 3	M<F (2.9)	2.1	0.5	2.2	–
U87960	Protein tyrosine phosphatase, receptor type, F (PTPRF); leukocyte common antigen receptor (LAR)	M<F (11.8)	–	0.1	–	0.4
AJ006971	DAP-like kinase (dlk)	M<F (6.4)	–	0.3	–	0.3
U08257 (X59996)	Glutamate receptor, ionotropic, kainite 4 (Grik4); Kainate receptor subunit (KA1)	M<F (5.8) (M<F (5.4))	– (–)	0.3 (0.2)	– (–)	0.5 (0.5)
AA892562	Dyskeratosis congenita 1, dyskerin (dkc1)	M<F (4.0)	–	0.4	–	0.4
X07686	L1Rn B6 repetitive DNA element	M<F (3.8)	2.0	0.4	–	0.2
X53455	Microtubule-associated protein 2 (MAP2)	M<F (3.5)	–	0.1	–	0.3
AA859593	EST, similar to mouse estrogen-responsive finger protein (efp)	M<F (3.4)	–	0.3	–	0.5
X17184	Glutamate receptor, ionotropic, AMPA subtype, GluR1	M<F (3.1)	–	0.3	–	0.5
AJ006295	Myeloid/lymphoid or mixed-lineage leukemia (trithorax (Drosophila) homolog); translocated to, 3 (mllt3); AF-9	–	–	0.4	–	0.5
AI231257	Cyclin D1	–	–	0.4	–	0.5
AA799791	Serine/threonine kinase 25 (STE20 homolog, yeast) (stk25)	–	–	0.4	–	0.4
U16845	Neurotrimin	–	–	0.5	–	0.5
AI639097	EST	–	–	2.2	–	0.5
AI176456	Metallothionein (MT1a)	M>F (2.8)	–	2.9	2.3	–

MPOA, medial preoptic area; EB, estradiol benzoate; FA, flutamide; M, males; F, females; EST, expressed sequence tag.

Figure 1. In the hypothalamus at PND 2, nuclear immunoreactivity of PARP, the protein product of the *adprt* gene (Skaper, 2003), was observed in the ventricular ependymal and subependymal cells around the third ventricle. On quantitative measurement of nuclear immunoreactivity at the SDN region, cases with higher grades of distribution were more frequent in female controls when compared with the males [Figs. 6(A,B) and 7]. EB-treatment increased and decreased the positive cell distribution in males and females, respectively [Figs. 6(C) and 7]. GluR1 immunoreactivity was observed in the cytoplasm and dendritic processes of neuronal cells, its staining intensity being mostly weak in the MPOAs, even in the positive cases, when compared with the other brain areas, such as the hippocampus, cerebral cortex, and striatum [Fig. 6(D)]. In the MPOAs of male controls, two out of four cases showed only minimal intensity of GluR1-immunoreactivity, and the other two showed negative results [Fig. 6(D), Table 6]. Although the intensity was minimal to slight, all control females showed positive immunoreactivity in their MPOAs [Fig. 6(E)]. EB-treatment did not alter the intensity in either sex [female: Fig. 6(F)]. With regard to GluR5, very faint immunoreactivity was observed in the dendritic processes in the striatum and bed nucleus, but staining was lacking in the MPOAs of both sexes, even with the EB treatment

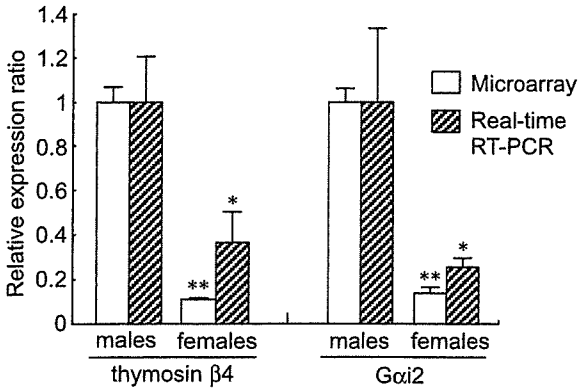

Figure 5 Confirmation of microarray data by real-time RT-PCR in the neonatal MPOA. Sex differences in the mRNA expression of thymosin $\beta 4$ and Gαi2 were analyzed. Significantly different from the male value in each detection system ($*p < 0.05$, $**p < 0.01$).

(Table 6). GluR6/7-immunoreactivity was observed in the cytoplasm of both neuronal and glial cells of the whole brain area, but there was no obvious change in terms of the distribution and intensity in the MPOAs, irrespective of the sex or EB treatment (Table 6). MAP2 immunoreactivity was observed in the whole dendritic processes with a fibrillary expression pattern, but there was no obvious change in terms of the distribution and intensity in the MPOAs, irrespective of the sex or EB treatment (Table 6). Strong cytoplasmic immunoreactivity of MT-1/2 was observed in the astrocytes located in the deep cortex and white matter of the cerebrum, hippocampal white matter, and striatum [Fig. 6(G)]. In other brain areas, MT-1/2-immunoreactivity was rather weak and sparse, and both nuclear and cytoplasmic. In the MPOAs, nuclear immunoreactivity predominated over cytoplasmic staining. On quantitative measurement of the nuclear immunoreactivity, the positive cell ratio was higher in males than in females, with increase in the latter on EB treatment [Figs. 6(G–I) and 7].

DISCUSSION

In the present validation study to establish a region-specific microarray analysis method using PET samples in combination with methacarn fixation, we found that gene expression profiles were very similar between 2×-amplified aRNAs from UFT and methacarn-fixed PET, and the deviation in expression data with the second-round amplification from the 1×-amplified aRNAs of UFT was mostly due to the preferential amplification of the 3′-terminal portion, irrespective of the tissue status. These results strongly indicate that methacarn fixation and subsequent paraffin embedding do not affect the expression fidelity in microarray analyses. Although it is still necessary to improve expression fidelity with second-round amplification, the results suggest an advantage of methacarn in combination with paraffin embedding for global gene expression analysis of microdissected cellular regions. It should be stressed that paraffin embedding is essential for preparation of serial sections necessary for microdissection of anatomically defined tissue areas.

Although the sex difference in the incidence of apoptosis in the SDN region that is believed to be re-

Figure 6 Immunoexpression patterns for PARP (panels A-C), GluR1 (panels D-F), and MT-1/2 (panels G-I), in the neonatal rat MPOA at PND 2. A. Note scattered PARP-immunoreactive nuclei (arrowheads) in paraventricular cells of a control male. The inset shows a high-power view of the nuclear weak immunoreactivity in the same area. B. Distribution of PARP-weakly immunoreactive cell nuclei in a control female. Note accumulation of positive cells in the SDN region (arrow). C. Lack of PARP-immunoreactive cells in most paraventricular and SDN regions in an EB-treated female. D. Very weak, mostly negative GluR1-immunoreactivity in the cytoplasmic processes of neurons in a control male. The inset shows strong immunoreactivity in the cytoplasm and dendritic processes of neuronal cells of the cerebral cortex of the same brain section. E. Slight intensity of GluR1-immunoreactivity in cytoplasmic processes of neurons in a control female. The inset shows a high-power view of the immunoreactivity in cytoplasmic processes of the same area. F. Minimal degree of GluR1-immunoreactivity in an EB-treated female. G. Diffuse immunoexpression of MT-1/2 in a control male. The expression pattern is mostly nuclear, and both astrocytic (arrowheads) and neuronal (arrows) populations as well as ependymal cells (*) show apparent immunoreactivity. The inset shows strong expression in cytoplasmic processes of astrocytes in the deep cerebral cortex of the same brain section. H. Scattered weak nuclear immunoreactivity of MT-1/2 in a control female. I. Diffuse nuclear and scattered cytoplasmic distribution of immunoreactive cells in an EB-treated female. The inset shows a high power view of both nuclear and cytoplasmic immunoreactivity in the same area. Bar = 50 μm, including insets.

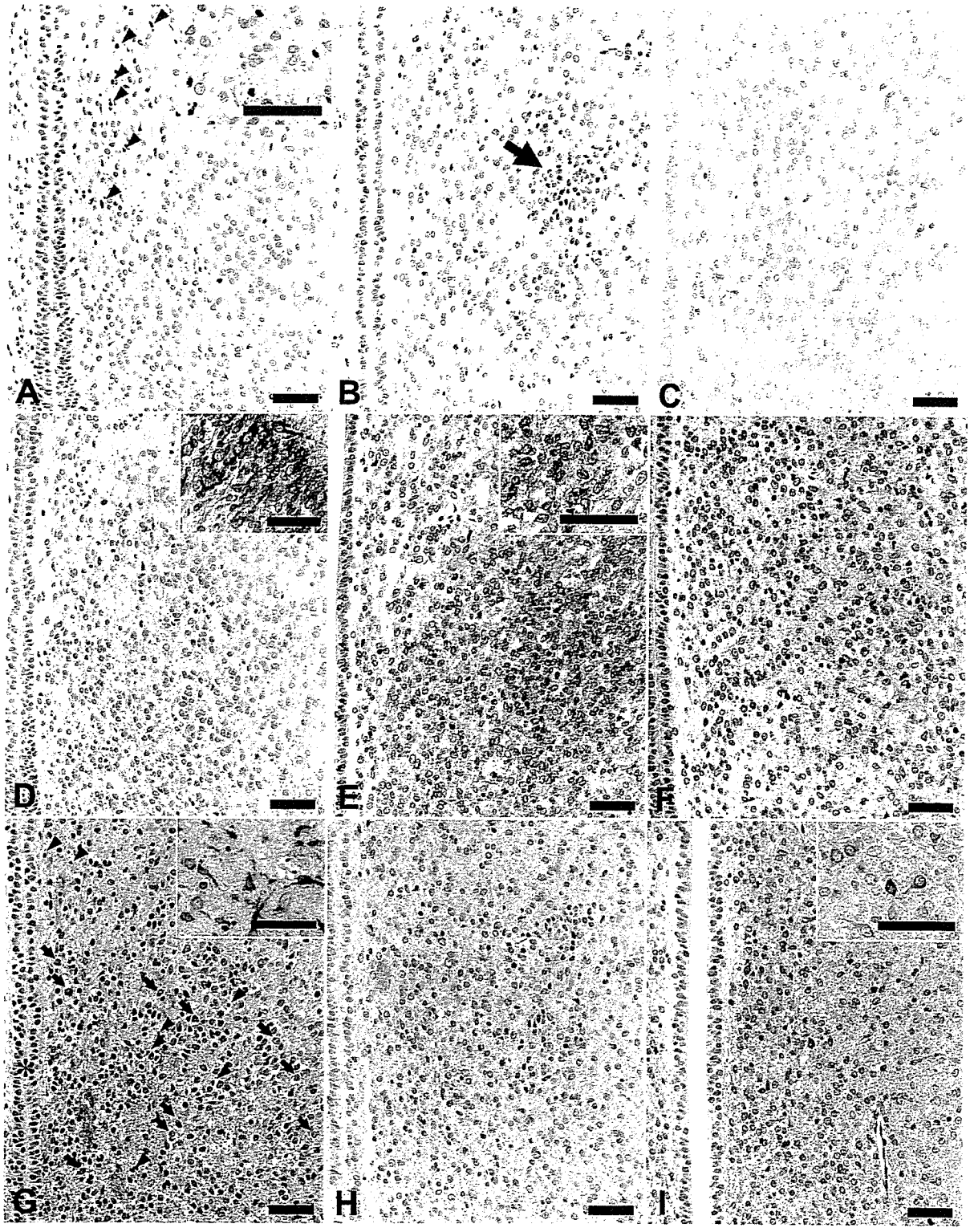

Figure 6

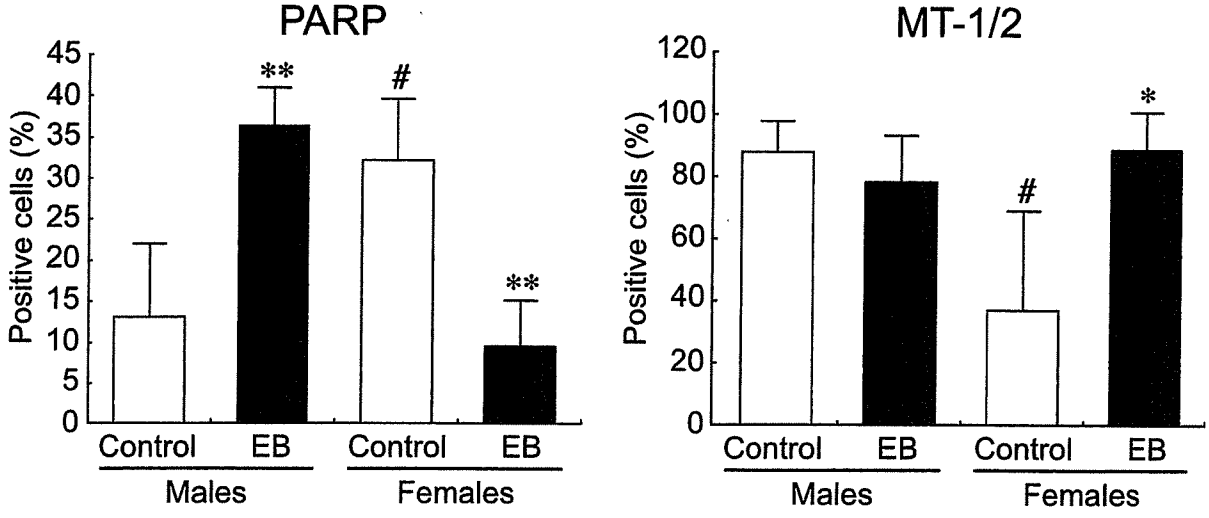

Figure 7 Nuclear immunoreactive cell percentages for PARP and MT-1/2 in neonatal rat MPOAs at PND 2. Significantly different from the corresponding controls ($*p < 0.05$, $**p < 0.01$). Significantly different from the male controls ($^{\#}p < 0.05$).

sponsible for subsequent sexually dimorphic development of this nucleus first occurs between PNDs seven and 10 (Davis et al., 1996), the number of genes exhibiting male-biased constitutive expression was much higher than in females at time points as early as PND 2 in the present study. This sex difference is presumably the reflection of growth and/or antiapoptotic effects for male-type large SDN under the influence of estradiol generated by aromatase from testosterone perinatally secreted from the developing testis (Matsumoto et al., 2000). Regarding responses to chemicals, the number of genes showing altered expression by EB or FA was far greater in females than in males, suggesting an effect on normal female sexual differentiation. Moreover, approximately 60% of genes showing male or female-biased expression demonstrated altered levels with EB in females, pointing to an involvement of genes necessary for normal processes of male- or female-type brain sexual differentiation in its disruptive effects. It is well known that the perinatal/neonatal treatment of animals with estrogenic compounds can affect sexual development of both sexes, resulting in reproductive dysfunction (Nagao et al., 1999; Odum et al., 2002; Tsukahara et al., 2003; Shibutani et al., 2005). With regard to the effects of antiandrogens, disruption of sexual development has generally been apparent in males, but the situation is largely unclear for females (Gray and Kelce, 1996; Wolf et al., 2004). With FA, however, prenatal exposure affects the volume of the anteroventral periventricular nucleus (AVPVN) in female rats (Lund et al., 2000) and the female sexual behavior in guinea pigs (Thornton et al., 1991). In addition, FA exerts antiprogestin activity (Chandrasekhar and Armstrong, 1989; Dukes et al., 2000).

Our search for genes showing altered expression by EB or FA revealed a total of four female-predominant genes with change by EB in both sexes, all up-regulated in males and down-regulated in females. Two of them are long interspersed repetitive DNAs, L1, or LINE, a class of mobile genetic elements named retrotransposons which can be amplified by retroposition, i.e. by a mechanism similar to that observed with retroviruses (Servomaa and Rytoamaa,

Table 6 Immunoreactivity of Protein Signals in the MPOA of Neonatal Rats Treated with EB[a]

	Males		Females	
Antigen	Control	EB	Control	EB
Number of animals	4	4	4	4
GluR1 (±/+)[b]	2[c](2/0)[d]	3(3/0)	4(3/1)	3(3/0)
GluR5 (present)	0	0	0	0
GluR6/7 (±/+/++)[b]	4(2/2/0)	4(0/4/0)	4(0/3/1)	4(2/2/0)
MAP2 (±/+/++)[b]	4(0/3/1)	4(0/3/1)	4(2/2/0)	4(2/2/0)

Protein signals with immunoexpression patterns for which morphometric analysis could not be applied were analyzed by visual estimation of the grade of intensity of immunoreactivity in the MPOA. MPOA, medial preoptic area; EB, estradiol benzoate; GluR1, glutamate receptor 1; GluR5, glutamate receptor 5; GluR6/7; glutamate receptor 6/7; MAP2, microtubule-associated protein 2.

[a]Rat neonates treated with EB at 10 μg/pup or vehicle on PND1 and sacrificed 24 h later were examined.

[b]Grades of intensity of immunoreactivity: ±, minimal; +, slight; ++, moderate; and +++, prominent.

[c]Total number of animals showing positive immunoreactivity.

[d]Number of animals with each grade.

1990). This group of retrotransposons includes regulatory signals and encodes two proteins, a RNA-binding protein and an integrase-replicase (Han and Boeke, 2005). The human genome contains about 500,000 LINES, accounting for roughly 17% of the total (Haoudi et al., 2004). Various environmental factors, such as steroid hormone-like agents and stressors can facilitate L1 transcription to alter cellular functions (Servomaa and Rytoamaa, 1990; Morales et al., 2002, 2003). Moreover, a regulatory role of L1 repeats at the promoter region has been reported with estrogen-related gene transcription (Hardy et al., 2001). During neuronal differentiation, retrotransposition events can alter the expression of neuronal genes, which, in turn, can influence neuronal cell fate (Muotri et al., 2005). Thus, the sex differences in the retrotransposon expression in the developing MPOA apparent here suggest roles in sex-dependent gene expression control, and alteration in their expression status due to EB may indicate roles as upstream regulators of genes necessary for brain sexual differentiation.

Two other genes showing up-regulation in males and down-regulation in females with EB, as well as female-biased expression, were *adprtl* and *NonO/p54nrb*. *Adprtl* encodes PARP-1, an abundant nuclear enzyme that is activated primarily by DNA damage; however, its excessive activation can lead to cell death (Skaper, 2003; Koh et al., 2005). Interestingly, sex differences exist regarding PARP-1 activation as well as nitric oxide toxicity in a mouse ischemic neurotoxicity model (McCullough et al., 2005). In the periventricular cell populations, poly(ADP-ribosyl)ation is basally activated by DNA strand breaks reflecting glutamate-nitric oxide neurotransmission (Pieper et al., 2000). In the present study, the measured level of PARP-immunoexpression at the SDN region was in line with the microarray data, suggesting an induction of subsequent programmed cell death in the female SDN-POA (Davis et al., 1996). Similarly, increased expression of PARP in males and its decrease in females with EB here may be linked to the decreased SDN volume in males in later life (Shibutani et al., 2005) and the decreased apoptosis in the female SDN after EB injection (Arai et al., 1996), respectively. NonO/p54nrb has been implicated in a variety of nuclear processes (Proteau et al., 2005). Indeed, this protein is known to act as a transcription factor necessary for adrenocortical steroidogenesis (Sewer et al., 2002), and as a transcriptional co-activator of the human androgen receptor (AR; Ishitani et al., 2003).

In the present study, a total of 15 genes exhibited altered expression due to FA in either sex, in addition to alteration by EB. Among them, 10 genes also exhibited sex differences in expression including the two genes for retrotransposons mentioned earlier. Interestingly, many of the 15 genes exhibited similar expression patterns with EB and FA, most being down-regulated in females, suggesting a common mechanism of action of the two chemicals. The following seven genes showed this particular expression pattern, in addition to the L1 repeat mentioned earlier: *PTPRF*/leukocyte common antigen-related (LAR) protein, *dlk*, two kinds of glutamate receptors, *dyskerin*, *MAP2*, and *efp*. In males, neonatal estrogen treatment affects the developing testis to suppress androgen secretion, presumably resulting in effects similar to antiandrogenicity on postnatal development (Atanassova et al., 1999). On the other hand, FA in the 20-day pubertal female assay using rats has been shown to exert ER-agonist activity on female sexual development, attributed to an imbalance between endogenous estrogenic and androgenic stimuli in the target organs (Kim et al., 2002).

Regarding glutamate receptors, mRNA expression of GluR1, the AMPA subtype found here with altered expression, is up-regulated in the AVPVN by estrogen in ovariectomized juvenile female rats (Gu et al., 1999). Hypothalamic GluR1 protein level was also increased in gonadectomized and estrogen-treated adult rats irrespective of the sex (Diano et al., 1997). Different from our female neonates, these results suggest that estrogen could up-regulate GluR1 levels in the juvenile/adult rat hypothalamus, probably through a different mechanism from that during sexual differentiation. In the female MPOA, we here could detect a slight, but nonsignificant increase in GluR1-immunoreactive cases when compared with those in males. Although we could not examine immunohistochemical localization of KA1 subunit here, other kainate receptor subtypes (GluR5, 6, and 7) have shown, in a study using adult rats, to be expressed in tanycytes, astrocytes, and neurons of the arcuate nucleus, with co-expression of AR or ER found in neurons in males and females, respectively (Diano et al., 1998). However, we could not detect any sex difference or EB-induced effect on the immunoreactivity of GluR5 or GluR6/7 in the neonatal MPOA.

PTPRF/LAR is a widely expressed tyrosine phosphatase that has been implicated in the regulation of a diverse range of signaling pathways, such as in the development and maintenance of excitatory synapses, and interestingly, disruption of its function results in reduction of surface AMPA receptors (Mooney and LeVea, 2003; Dunah et al., 2005). In the present study, AMPA subtype GluR1, as mentioned earlier, showed similar responses to EB and FA as well as a sex differ-

ence in mRNA expression, suggesting a coordinated action of PTPRF/LAR and AMPA receptors during brain sexual differentiation and its disruption.

MAP2 contributes to regulation of cytoskeletal organization and dynamics, and is expressed mainly in dendritic processes of neurons (Maccioni and Cambiazo, 1995). Posttranscriptional control of MAP2 expression has been reported in the female rat hippocampus in response to estrogen treatment or during the estrous cycle (Reyna-Neyra et al., 2002, 2004). Interestingly, estrogen can induce dendrite spines in the developing rat POA through activation of AMPA-kainate receptors by glutamate that may originate from astrocytes (Amateau and McCarthy, 2002). Inconsistent with the microarray data, MAP2-immunoreactivity in the neonatal MPOA here lacked any sex difference or change in expression on chemical treatment as in the case with above-mentioned GluR5 and GluR6/7.

Efp, a target gene product of ERα, is a RING-finger-dependent ubiquitin ligase that targets proteolysis of 14-3-3σ, a negative cell cycle regulator that causes G2 arrest (Urano et al., 2002), and is considered essential for estrogen-dependent tumor cell proliferation (Horie et al., 2003). This gene product is distributed mainly in estrogen-sensitive organs/tissues associated with ER co-expression (Orimo et al., 1995; Shimada et al., 2004). Dlk is a nuclear serine/threonine-specific kinase that has been implicated in the regulation of apoptosis by relocation to the cytoplasm, but its nuclear location has been suggestive of the roles for mitosis and cytokinesis (Preuss et al., 2003). Dyskerin, a nucleolar protein that modifies specific uridine residues of rRNA, also acting as a component of the telomerase complex, is a target molecule for skin and bone marrow failure syndrome called dyskeratosis congenita in human (Marrone et al., 2005). Dyskerin transcripts distribute ubiquitously in embryo-fetal tissues with notably high levels in epithelial and neural tissues (Heiss et al., 2000).

As a unique gene showing male-biased expression and increase with EB in females and decrease with FA in males, *MT1a* is of interest. MTs are considered to be important metal-binding proteins active in defense against heavy metal toxicity (Sogawa et al., 2001), and four major MT isoforms have so far been identified. In the present study, judging from the sequence information (accession no. AI176456) for the MT probes, either MT1 or 2 was suggested to be responsible for the particular expression pattern. Sex steroid-related expression changes in MT1 and/or 2 have been reported in the liver or brain of mice (Sogawa et al., 2001; Beltramini et al., 2004). In the brain, MT1 and 2 are expressed mainly in nonneuronal cells (Suzuki et al., 1994; Hidalgo et al., 2001), but certain levels are also found in neurons (Xie et al., 2004); as well as cytoplasmic expression, nuclear localization of MT has been reported in developing brain (Suzuki et al., 1994). Interestingly, kainic acid treatment can selectively induce MT1 in neurons and MT2 in glial cells in rats (Kim et al., 2003). Although the immunoreactivity of MT-1/2 was rather weak when compared with other brain areas and a nuclear expression was predominant in the neonatal MPOA here, male predominance may reflect a neuroprotective function, and expression changes due to EB and FA could indicate alteration in the regional hormonal environment in response to treatment.

In summary, we here established the basis for a global gene expression profiling method using paraffin-embedded, histologically defined small tissue areas with methacarn as a fixative. A male predominance in the number of genes showing constitutively higher expression suggestive of sex steroidal effects on the neonatal male MPOA was detected. Upon treatment with EB, many genes showing sex differences in expression demonstrated altered levels in females, in line with involvement of genes necessary for brain sexual differentiation in its disruption. Moreover, many genes commonly affected by EB and FA showed down-regulation in females with these drugs, suggesting common mechanisms shared between estrogenic and anti-androgenic chemicals in induction of endocrine center disruption in females, at least in early stages.

We thank Mrs. Keiko Kuroiwa for her technical assistance in conducting the immunohistochemical study. Dr. Lee was an Awardee of a Postdoctoral Fellowship from the Japan Society for the Promotion of Science during the performance of the study.

REFERENCES

Amateau SK, McCarthy MM. 2002. A novel mechanism of dendritic spine plasticity involving estradiol induction of prostaglandin-E_2. J Neurosci 22:8586–8596.

Arai Y, Sekine Y, Murakami S. 1996. Estrogen and apoptosis in the developing sexually dimorphic preoptic area in female rats. Neurosci Res 25:403–407.

Atanassova N, McKinnell C, Walker M, Turner KJ, Fisher JS, Morley M, Millar MR, et al. 1999. Permanent effects of neonatal estrogen exposure in rats on reproductive hormone levels, Sertoli cell number, and the efficiency of spermatogenesis in adulthood. Endocrinology 140:5364–5373.

Beltramini M, Zambenedetti P, Wittkowski W, Zatta P. 2004. Effects of steroid hormones on the Zn, Cu and MTI/II levels in the mouse brain. Brain Res 1013:134–141.

Chandrasekhar Y, Armstrong DT. 1989. Ability of progesterone to reverse anti-androgen (hydroxyflutamide)-induced interference with the preovulatory LH surge and ovulation in PMSG-primed immature rats. J Reprod Fertil 85:309–316.

Davis EC, Popper P, Gorski RA. 1996. The role of apoptosis in sexual differentiation of the rat sexually dimorphic nucleus of the preoptic area. Brain Res 734:10–18.

Diano S, Naftolin F, Horvath TL. 1997. Gonadal steroids target AMPA glutamate receptor-containing neurons in the rat hypothalamus, septum and amygdala: A morphological and biochemical study. Endocrinology 138:778–789.

Diano S, Naftolin F, Horvath TL. 1998. Kainate glutamate receptors (GluR5-7) in the rat arcuate nucleus: Relationship to tanycytes, astrocytes, neurons and gonadal steroid receptors. J Neuroendocrinol 10:239–247.

Dukes M, Furr BJ, Hughes LR, Tucker H, Woodburn JR. 2000. Nonsteroidal progestins and antiprogestins related to flutamide. Steroids 65:725–731.

Dunah AW, Hueske E, Wyszynski M, Hoogenraad CC, Jaworski J, Pak DT, Simonetta A, et al. 2005. LAR receptor protein tyrosine phosphatases in the development and maintenance of excitatory synapses. Nat Neurosci 8:458–467.

Gray LE Jr, Kelce WR. 1996. Latent effects of pesticides and toxic substances on sexual differentiation of rodents. Toxicol Ind Health 12:515–531.

Gu G, Varoqueaux F, Simerly RB. 1999. Hormonal regulation of glutamate receptor gene expression in the anteroventral periventricular nucleus of the hypothalamus. J Neurosci 19:3213–3222.

Han JS, Boeke JD. 2005. LINE-1 retrotransposons: Modulators of quantity and quality of mammalian gene expression? Bioessays 27:775–784.

Haoudi A, Semmes OJ, Mason JM, Cannon RE. 2004. Retrotransposition-competent human LINE-1 induces apoptosis in cancer cells with intact p53. J Biomed Biotechnol 2004:185–194.

Hardy DO, Niu EM, Catterall JF. 2001. Kap promoter analysis *in vivo*: A regulatory role for a truncated L1 repeat. Mol Cell Endocrinol 181:57–67.

Heiss NS, Bächner D, Salowsky R, Kolb A, Kioschis P, Poustka A. 2000. Gene structure and expression of the mouse dyskeratosis congenita gene, *dkc1*. Genomics 67: 153–163.

Hidalgo J, Aschner M, Zatta P, Vasak M. 2001. Roles of the metallothionein family of proteins in the central nervous system. Brain Res Bull 55:133–145.

Horie K, Urano T, Ikeda K, Inoue S. 2003. Estrogen-responsive RING finger protein controls breast cancer growth. J Steroid Biochem Mol Biol 85:101–104.

Ishitani K, Yoshida T, Kitagawa H, Ohta H, Nozawa S, Kato S. 2003. p54nrb acts as a transcriptional coactivator for activation function 1 of the human androgen receptor. Biochem Biophys Res Commun 306:660–665.

Kim D, Kim EH, Kim C, Sun W, Kim HJ, Uhm CS, Park SH, et al. 2003. Differential regulation of metallothionein-I, II, and III mRNA expression in the rat brain following kainic acid treatment. Neuroreport 14:679–682.

Kim HS, Shin JH, Moon HJ, Kim TS, Kang IH, Seok JH, Kim IY, et al. 2002. Evaluation of the 20-day pubertal female assay in Sprague-Dawley rats treated with DES, tamoxifen, testosterone, and flutamide. Toxicol Sci 67: 52–62.

Kocarek TA, Kraniak JM, Reddy AB. 1998. Regulation of rat hepatic cytochrome P450 expression by sterol biosynthesis inhibition: Inhibitors of squalene synthase are potent inducers of CYP2B expression in primary cultured rat hepatocytes and rat liver. Mol Pharmacol 54:474–484.

Koh DW, Dawson TM, Dawson VL. 2005. Poly(ADP-ribosyl)ation regulation of life and death in the nervous system. Cell Mol Life Sci 62:760–768.

Lund TD, Salyer DL, Fleming DE, Lephart ED. 2000. Pre or postnatal testosterone and flutamide effects on sexually dimorphic nuclei of the rat hypothalamus. Brain Res Dev Brain Res 120:261–266.

Maccioni RB, Cambiazo V. 1995. Role of microtubule-associated proteins in the control of microtubule assembly. Physiol Rev 75:835–864.

Marrone A, Walne A, Dokal I. 2005. Dyskeratosis congenita: Telomerase, telomeres and anticipation. Curr Opin Genet Dev 15:249–257.

Masutomi N, Shibutani M, Takagi H, Uneyama C, Takahashi N, Hirose M. 2003. Impact of dietary exposure to methoxychlor, genistein, or diisononyl phthalate during the perinatal period on the development of the rat endocrine/reproductive systems in later life. Toxicology 192: 149–170.

Matsumoto A, Sekine Y, Murakami S, Arai Y. 2000. Sexual differentiation of neuronal circuitry in the hypothalamus. In: Matsumoto A, editor. Sexual Differentiation of the Brain. Boca Raton: CRC Press, pp 203–227.

McCullough LD, Zeng Z, Blizzard KK, Debchoudhury I, Hurn PD. 2005. Ischemic nitric oxide and poly (ADP-ribose) polymerase-1 in cerebral ischemia: Male toxicity, female protection. J Cereb Blood Flow Metab 25:502–512.

McEwen BS, Alves SE. 1999. Estrogen actions in the central nervous system. Endocr Rev 20:279–307.

Meisel RL, Sachs BD. 1994. The physiology of male sexual behavior. In: Knobil E, Neills JD, editors. The Physiology of Reproduction, 2nd ed. New York: Raven Press, pp 3–106.

Meredith JM, Bennett C, Scallet AC. 2001. A practical three-dimensional reconstruction method to measure the volume of the sexually-dimorphic central nucleus of the medial preoptic area (MPOC) of the rat hypothalamus. J Neurosci Methods 104:113–121.

Mooney RA, LeVea CM. 2003. The leukocyte common antigen-related protein LAR: Candidate PTP for inhibitory targeting. Curr Top Med Chem 3:809–819.

Morales JF, Snow ET, Murnane JP. 2002. Environmental factors affecting transcription of the human L1 retrotransposon. I. Steroid hormone-like agents. Mutagenesis 17:193–200.

Morales JF, Snow ET, Murnane JP. 2003. Environmental factors affecting transcription of the human L1 retrotransposon. II. Stressors. Mutagenesis 18:151–158.

Muotri AR, Chu VT, Marchetto MC, Deng W, Moran JV, Gage FH. 2005. Somatic mosaicism in neuronal precursor cells mediated by L1 retrotransposition. Nature 435:903–910.

Nagao T, Saito Y, Usumi K, Kuwagata M, Imai K. 1999. Reproductive function in rats exposed neonatally to bisphenol A and estradiol benzoate. Reprod Toxicol 13:303–311.

Numan M. 1994. Maternal behavior. In: Knobil E, Neills JD, editors. The Physiology of Reproduction, 2nd ed. New York: Raven Press, pp 221–302.

Odum J, Lefevre PA, Tinwell H, Van Miller JP, Joiner RL, Chapin RE, Wallis NY, et al. 2002. Comparison of the developmental and reproductive toxicity of diethylstilbestrol administered to rats *in utero*, lactationally, preweaning, or postweaning. Toxicol Sci 68:147–163.

Orikasa C, Kondo Y, Hayashi S, McEwen BS, Sakuma Y. 2002. Sexually dimorphic expression of estrogen receptor β in the anteroventral periventricular nucleus of the rat preoptic area: Implication in luteinizing hormone surge. Proc Natl Acad Sci USA 99:3306–3311.

Orimo A, Inoue S, Ikeda K, Noji S, Muramatsu M. 1995. Molecular cloning, structure, and expression of mouse estrogen-responsive finger protein Efp. Co-localization with estrogen receptor mRNA in target organs. J Biol Chem 270:24406–24413.

Pieper AA, Blackshaw S, Clements EE, Brat DJ, Krug DK, White AJ, Pinto-Garcia P, et al. 2000. Poly(ADP-ribosyl) ation basally activated by DNA strand breaks reflects glutamate-nitric oxide neurotransmission. Proc Natl Acad Sci USA 97:1845–1850.

Preuss U, Bierbaum H, Buchenau P, Scheidtmann KH. 2003. DAP-like kinase, a member of the death-associated protein kinase family, associates with centrosomes, centromers, and the contractile ring during mitosis. Eur J Cell Biol 82:447–459.

Proteau A, Blier S, Albert AL, Lavoie SB, Traish AM, Vincent M. 2005. The multifunctional nuclear protein p54nrb is multiphosphorylated in mitosis and interacts with the mitotic regulator Pin1. J Mol Biol 346:1163–1172.

Reyna-Neyra A, Arias C, Ferrera P, Morimoto S, Camacho-Arroyo I. 2004. Changes in the content and distribution of microtubule associated protein 2 in the hippocampus of the rat during the estrous cycle. J Neurobiol 60:473–480.

Reyna-Neyra A, Camacho-Arroyo I, Ferrera P, Arias C. 2002. Estradiol and progesterone modify microtubule associated protein 2 content in the rat hippocampus. Brain Res Bull 58:607–612.

Rhees RW, Shryne JE, Gorski RA. 1990a. Onset of the hormone-sensitive perinatal period for sexual differentiation of the sexually dimorphic nucleus of the preoptic area in female rats. J Neurobiol 21:781–786.

Rhees RW, Shryne JE, Gorski RA. 1990b. Termination of the hormone-sensitive period for differentiation of the sexually dimorphic nucleus of the preoptic area in male and female rats. Dev Brain Res 52:17–23.

Rivas A, Fisher JS, McKinnell C, Atanassova N, Sharpe RM. 2002. Induction of reproductive tract developmental abnormalities in the male rat by lowering androgen production or action in combination with a low dose of diethylstilbestrol: Evidence for importance of the androgen-estrogen balance. Endocrinology 143:4797–4808.

Servomaa K, Rytomaa T. 1990. UV light and ionizing radiations cause programmed death of rat chloroleukaemia cells by inducing retropositions of a mobile DNA element (L1Rn). Int J Radiat Biol 57:331–343.

Sewer MB, Nguyen VQ, Huang CJ, Tucker PW, Kagawa N, Waterman MR. 2002. Transcriptional activation of human CYP17 in H295R adrenocortical cells depends on complex formation among p54nrb/NonO, protein-associated splicing factor, and SF-1, a complex that also participates in repression of transcription. Endocrinology 143:1280–1290.

Shibutani M, Masutomi N, Uneyama C, Abe N, Takagi H, Lee KY, Hirose M. 2005. Down-regulation of GAT-1 mRNA expression in the microdissected hypothalamic medial preoptic area of rat offspring exposed maternally to ethinylestradiol. Toxicology 208:35–48.

Shibutani M, Uneyama C. 2002. Methacarn: A fixation tool for multipurpose genetic analysis from paraffin-embedded tissues. In: Conn M, editor. Methods in Enzymology, Vol. 356. New York: Academic Press, pp 114–125.

Shibutani M, Uneyama C, Miyazaki K, Toyoda K, Hirose M. 2000. Methacarn fixation: A novel tool for analysis of gene expressions in paraffin-embedded tissue specimens. Lab Invest 80:199–208.

Shimada N, Suzuki T, Inoue S, Kato K, Imatani A, Sekine H, Ohara S, et al. 2004. Systemic distribution of estrogen-responsive finger protein (Efp) in human tissues. Mol Cell Endocrinol 218:147–153.

Skaper SD. 2003. Poly(ADP-ribose) polymerase-1 in acute neuronal death and inflammation: A strategy for neuroprotection. Ann NY Acad Sci 993:217–228; discussion 287–288.

Sogawa N, Sogawa CA, Oda N, Fujioka T, Onodera K, Furuta H. 2001. The effects of ovariectomy and female sex hormones on hepatic metallothionein-I gene expression after injection of cadmium chloride in mice. Pharmacol Res 44:53–57.

Suzuki K, Nakajima K, Otaki N, Kimura M. 1994. Metallothionein in developing human brain. Biol Signals 3:188–192.

Takagi H, Shibutani M, Kato N, Fujita H, Lee KY, Takigami S, Mitsumori K, et al. 2004. Microdissected region-specific gene expression analysis with methacarn-fixed, paraffin-embedded tissues by real-time RT-PCR. J Histochem Cytochem 52:903–913.

Tena-Sempere M, Gonzalez LC, Pinilla L, Huhtaniemi I, Aguilar E. 2001. Neonatal imprinting and regulation of estrogen receptor α and β mRNA expression by estrogen in the pituitary and hypothalamus of the male rat. Neuroendocrinology 73:12–25.

Thornton JE, Irving S, Goy RW. 1991. Effects of prenatal antiandrogen treatment on masculinization and defeminization of Guinea pigs. Physiol Behav 50: 471–475.

Tsukahara S, Ezawa N, Yamanouchi K. 2003. Neonatal estrogen decreases neural density of the septum-midbrain central gray connection underlying the lordosis-inhibiting system in female rats. Neuroendocrinology 78:226–233.

Uneyama C, Shibutani M, Masutomi N, Takagi H, Hirose M. 2002. Methacarn fixation for genomic DNA analysis in microdissected, paraffin-embedded tissue specimens. J Histochem Cytochem 50:1237–1245.

Urano T, Saito T, Tsukui T, Fujita M, Hosoi T, Muramatsu M, Ouchi Y, et al. 2002. Efp targets 14-3-3σ for proteolysis and promotes breast tumour growth. Nature 417: 871–875.

Wolf CJ, LeBlanc GA, Gray LE Jr. 2004. Interactive effects of vinclozolin and testosterone propionate on pregnancy and sexual differentiation of the male and female SD rat. Toxicol Sci 78:135–143.

Xie T, Tong L, McCann UD, Yuan J, Becker KG, Mechan AO, Cheadle C, et al. 2004. Identification and characterization of metallothionein-1 and -2 gene expression in the context of (±)3, 4-methylenedioxymethamphetamine-induced toxicity to brain dopaminergic neurons. J Neurosci 24:7043–7050.

MOLECULAR CARCINOGENESIS 42:9–17 (2005)

In Vivo Mutational Analysis of Liver DNA in *gpt* Delta Transgenic Rats Treated With the Hepatocarcinogens *N*-Nitrosopyrrolidine, 2-Amino-3-Methylimidazo[4,5-*f*]Quinoline, and Di(2-Ethylhexyl)Phthalate

Keita Kanki,[1] Akiyoshi Nishikawa,[1]* Ken-ichi Masumura,[2] Takashi Umemura,[1] Takayoshi Imazawa,[1] Yasuki Kitamura,[1] Takehiko Nohmi,[2] and Masao Hirose[1]

[1]*Division of Pathology, National Institute of Health Sciences, Setagaya-ku, Tokyo, Japan*
[2]*Division of Genetics and Mutagenesis, National Institute of Health Sciences, Setagaya-ku, Tokyo, Japan*

In order to cast light on carcinogen-specific molecular mechanisms underlying experimental hepatocarcinogenesis in rats, in vivo mutagenicity and mutation spectra of known genotoxic rat hepatocarcinogens *N*-nitrosopyrrolidine (NPYR), and 2-amino-3-methylimidazo[4,5-*f*]quinoline (IQ), as well as the nongenotoxic hepatocarcinogen di(2-ethylhexyl)phthalate (DEHP) and the noncarcinogen acetaminophen (AAP), were investigated in guanine phosphoribosyltransferase (*gpt*) delta transgenic rats, a recently developed animal model for genotoxicity analysis. After 13-wk treatment, glutathione *S*-transferase placental form (GST-P)-positive liver cell foci were significantly increased in NPYR-treated and IQ-treated rats. In the DEHP-treated rats, marked hepatomegaly with centrilobular hypertrophy of hepatocytes occurred, although GST-P staining was consistently negative. Positive mutagenicity was detected in IQ- and NPYR-treated rats. Mutant frequencies (MFs) in the liver DNA were 188.0×10^{-6} and 56.5×10^{-6}, approximately 35-fold and 10-fold higher, respectively, than that of nontreatment control rats (5.5×10^{-6}). There were no increases in MFs in the DEHP- or AAP-treated rats as compared to the nontreatment control value. IQ induced mainly base substitutions leading to G:C to T:A transversions (56.9%) and deletions of G:C base pairs. In contrast, NPYR primarily caused specific A:T to G:C transitions (49.3%), which are very rare in the other groups. These data provided support for the conclusion that IQ and NPYR hepatocarcinogenesis depends on genotoxic processes and specific DNA adduct formation while DEHP exerts its influence via a nongenotoxic promotional pathway. Our data also indicate that analysis of specific in vivo mutational responses with transgenic animal models can provide crucial information for understanding the molecular mechanisms underlying chemical carcinogenesis.

Key words: hepatocarcinogens; in vivo mutation assay; *gpt* delta rats

INTRODUCTION

Environmental carcinogens are classified into genotoxic and nongenotoxic types based on in vitro bacterial mutagenicity. However, it is well-documented that in vitro mutagenicity does not always reflect in vivo mutagenicity and carcinogenicity in rodents [1–4]. The discrepancy between in vivo and in vitro models may result from organ-specific pathways of xenobiotic metabolism and DNA repair in vivo. To accomplish in vivo detection of gene mutations in multiple organs, transgenic rodents carrying reporter genes such as *lacI*, *lacZ*, and guanine phosphoribosyltransferase (*gpt*) have been developed [5]. These model animals can provide crucial information for understanding the in vivo mechanism of organ-specific mutagenesis induced by various carcinogens present in the human environment.

In spite of the toxicological importance of rat species, in vivo mutagenicity has been extensively studied in transgenic mice because of their availability. Recently, a novel transgenic rodent for genotoxicity analysis, named the *gpt* delta rat, has been developed [6]. Advantageous features allow positive detection of different types of mutations, including point mutations and deletions, as also shown with *gpt* delta mice [7]. Point mutations are

Abbreviations: *gpt*, guanine phosphoribosyltransferase; 6-TG, 6-thioguanine; NPYR, *N*-nitrosopyrrolidine; IQ, 2-amino-3-methylimidazo[4,5-*f*]quinoline; DEHP, di(2-ethylhexyl)phthalate; AAP, acetaminophen; MEHP, mono(2-ethylhexyl)phthalate; 8-OHdG, 8-hydroxydeoxyguanosine; MF, mutant frequency; GST-P, glutathione *S*-transferase placental form.

*Correspondence to: Division of Pathology, National Institute of Health Sciences, 1-18-1 Kamiyoga, Setagaya-ku, Tokyo 158-8501, Japan.

Received 21 May 2004; Revised 22 July 2004; Accepted 24 August 2004

DOI 10.1002/mc.20061

detected by 6-thioguanine (6-TG) selection with the *gpt* gene of *E. coli* and deletion mutations are identified by Spi$^-$ selection with the *red/gam* genes of lambda phage [5]. In the present study, aimed at elucidating carcinogen-specific mutagenic mechanisms underlying experimental hepatocarcinogenesis, in vivo mutation spectrum of *N*-nitrosopyrrolidine (NPYR), a carcinogenic cyclic nitrosamine present in processed food and tobacco smoke in the human environment [8,9], was investigated in *gpt* delta rats. NPYR is metabolically activated by microsomal P450, and its metabolites have been shown to form guanine adducts mainly, due to simple alkylation in the in vitro system [10]. The in vitro mutagenicity is detected only in the presence of an activating system such as rat liver homogenate [11]. Although the bacterial systems with *lacI* gene and M13mp2 phage DNA have shown the predominant base substitutions at G:C base pair [12,13], the in vivo mutation spectrum of NPYR has not yet been determined. Therefore, with *gpt* delta rats, the present study aimed to elucidate the in vivo mechanism of mutagenesis induced by NPYR in comparison with the mutation spectra of other hepatocarcinogens. For this purpose, well-studied rodent hepatocarcinogens 2-amino-3-methylimidazo[4,5-*f*]quinoline (IQ) and di(2-ethylhexyl)phthalate (DEHP) were also subjected to the in vivo mutation assay. In addition, a nonmutagenic hepatotoxic compound, acetaminophen (AAP), was used as a negative control chemical for the mutagenicity assay.

Heterocyclic aromatic amines are the major class of genotoxic hepatocarcinogens in rodents, as well as *N*-nitroso compounds, which may be active in humans [14,15]. IQ is one of the most carcinogenic and mutagenic heterocyclic aromatic amine present in cooked-foods and cigarette smoke [14,16]. In rodents, it exerts multipotential carcinogenicity in various organs [17], including the liver of nonhuman primates [18]. Potent mutagenicity with DNA adduct formation has been shown both in vitro and in vivo [19] and mutational analysis conducted in BigBlue rats has revealed characteristic G:C transversions and 1 bp G:C deletions in the liver, colon, and kidney [20]. Thus, because of abundant background data of carcinogenicity and mutagenicity, IQ can be used as an appropriate standard mutagen for the mutational analysis.

DEHP is a widely used plasticizer for vinylchloride products, which has been found to cause liver tumors in rats and mice in long-term feeding assays [21]. Because no mutagenicity has been detected in in vitro mutagenicity tests [22,23], DEHP has been categorized as a nongenotoxic carcinogen. However, several studies have suggested possible mutagenicity of mono(2-ethylhexyl)phthalate (MEHP), a principal hydrolysis metabolite of DEHP, in the reverse mutation assay (*E. coli*) and the Rec$^-$ assay (*B. subtilis*) [24,25]. Moreover, significant increases of 8-hydroxydeoxyguanosine (8-OHdG), a premutagenic DNA adduct formed by oxidative stress, have been observed in hepatic DNA of rats treated with DEHP, suggesting the involvement of oxidative DNA damage in its hepatocarcinogenesis [26,27]. Thus, in the present study DEHP was included in order to clarify its in vivo mutagenicity in the *gpt* delta system, which can widely and efficiently detect both point mutations and deletions with two different types of selection.

Accumulated studies have suggested that the transgenic animals are useful models for evaluating carcinogenic risk and chemopreventive potential of environmental materials to which humans are exposed [28–30]. Moreover, analyses of mutation spectra provide important information for understanding the molecular mechanisms underlying chemical carcinogenesis [31]. In the present study, in vivo mutagenicity analyses of major classes of rodent hepatocarcinogens were, therefore, performed in *gpt* delta rats and their possible mechanisms of hepatocarcinogenesis are discussed.

MATERIALS AND METHODS

Animals and Treatments

Twenty-five female Sprague-Dawley *gpt* delta rats carrying about ten tandem copies of the transgene lambda EG10 per haploid genome obtained from Japan SLC (Shizuoka, Japan) were randomized by weight into five groups. They were housed in a room with a barrier system, and maintained under the following constant conditions: temperature of 24 ± 1°C, relative humidity of 55 ± 5%, ventilation frequency of 18 times/h, and a 12 h light-dark cycle with free access to Oriental MF basal diet (Oriental Yeast Co., Ltd., Tokyo, Japan) and tap water.

Starting at 11-wk of age the rats were treated with test chemicals or maintained as controls for 13 wk. Groups of five animals were fed IQ (Toronto Research Chemical, Inc., Ont., Canada), DEHP (Wako Pure Chemical, Osaka, Japan), and AAP (Sigma Chemical Co., St. Louis, MO) at doses of 300, 12000, and 10000 ppm in MF basal diet, respectively. Another five rats were given NPYR (Aldrich Chemical Co., Milwaukee, WI) dissolved in a small quantity of ethanol and diluted in their drinking water at a dose of 200 ppm. The five nontreatment control rats received MF basal diet alone and tap water. At the end of the experiment, all animals were killed, and a part of the left lateral lobe of the liver was preserved at −80°C for subsequent in vivo mutation assays. The rest of the lobes were fixed in 10% buffered formalin for histopathological examination. Immunostaining of glutathione *S*-transferase placental form (GST-P) was performed by using polyclonal anti-GST-P (MBL, Nagoya, Japan) as the primary antibody, and goat IgG raised against rabbit

IgG as the secondary antibody. The signals were amplified with ABC KIT (DAKO, Kyoto, Japan), and detected with 3,3′-diaminobenzidine (DAB). The numbers and areas of GST-P positive liver cell foci comprising ten or more cells were measured by using an Image Processor for Analytical Pathology (IPAP, Sumika Technos, Osaka, Japan).

In Vivo Mutation Assays

The 6-TG and Spi$^-$ selections were performed as previously described [5]. Briefly, genomic DNA was extracted from the liver, and lambda EG10 DNA (48 kb) was rescued as the lambda phage by in vitro packaging. For 6-TG selection, the packaged phage was incubated with *E. coli* YG6020, which expresses Cre recombinase, and converted to a plasmid carrying *gpt* and chloramphenicol acetyltransferase. Infected cells were mixed with molten soft agar and poured onto agar plates containing chloramphenicol and 6-TG. In order to determine the total number of rescued plasmids, 3000-fold diluted phages were used to infect YG6020, and were poured on the plates containing chloramphenicol without 6-TG. The plates were incubated at 37°C for the selection of 6-TG-resistant colonies. Positively selected colonies were counted on d 3 and collected on d 4. The MF was calculated by dividing the number of *gpt* mutants after clonal correction by the number of rescued phages.

For the Spi$^-$ selection, the packaged phage was incubated with *E. coli* XL-1 Blue MRA for survival titration and *E. coli* XL-1 Blue MRA P2 for mutant selection. Infected cells were mixed with molten lambda-trypticase soft agar and poured onto lambda-trypticase agar plates. Next day, plaques (Spi$^-$ candidates) were punched out with sterilized glass pipettes and the agar plugs were suspended in SM buffer. In order to confirm the Spi$^-$ phenotype of candidates, the suspensions were spotted on three types of plates where XL-1 Blue MRA, XL-1 Blue MRA P2, or WL95 P2 strains were spread with soft agar. The real Spi$^-$ mutants, which made clear plaques on every plate, were collected and stored as phage lysates at 4°C. Approximate deletion sizes of the Spi$^-$ mutants were determined by agarose gel electrophoresis of the PCR-amplified target sequence.

For characterizing the mutation spectra of *gpt* mutants, a 739 bp DNA fragment containing the 456 bp coding region of the *gpt* gene was amplified by PCR as described previously [5]. DNA sequencing was performed with Big Dye™ Terminater Cycle Sequencing Ready Reaction (Applied Biosystems, Foster City, CA) on an ABI PRISM™ 310 Genetic Analyzer (Applied Biosystems).

Statistical Evaluation

For statistical analysis, the Student's *t*-test was used to compare liver and body weights, and quantitative data for GST-P positive liver cell foci and MFs between groups.

RESULTS

Growth of Animals, Liver Weights, and Chemical Intake

Data for final body and organ weights, and intake of test chemicals are shown in Table 1. The final body weight was not affected by any treatment during the experiment. Daily intakes of IQ, NPYR, and DEHP calculated from the consumption of diet or water were comparable to those in previous studies which showed significant carcinogenicity in rats [8,17,21]. Liver/body weight ratios were significantly ($P < 0.01$) increased in all rats that received chemicals, suggesting sufficient dosing. Especially, marked hepatomegaly was observed in the DEHP-treated rats ($P < 0.01$) with an increase to 183% of the nontreatment control value.

Histopathology and Immunohistochemical Analysis of GST-P

Histopathologically altered, mostly clear, hepatocellular foci were frequently observed in the IQ-treated and NPYR-treated rats (Figure 1A and C).

Table 1. Body and Liver Weights, and Food, Water, and Chemical Intake Data

Treatment	Number of rats	Body weight (g)[a]	Liver/body weight ratio (%)[a]	Food intake (g/rat/d)	Water intake (mL/rat/d)	Chemical intake	
						Total (mg/rat)	Daily (mg/rat/d)
IQ	5	264.6 ± 22.7	3.32 ± 0.11*	14.3	—	362	4.0
NPYR	5	257.8 ± 10.9	3.25 ± 0.16*	13.6	17.1	310	3.4
DEHP	5	279.3 ± 36.6	4.98 ± 0.28**	14.0	—	17 010	187.0
AAP	5	266.5 ± 11.4	3.40 ± 0.29*	15.6	—	12 740	140.0
Control	5	269.6 ± 27.0	2.72 ± 0.21	13.3	23.2	—	—

IQ, 2-amino-3-methylimidazo[4,5-*f*]quinoline; NPYR, *N*-nitrosopyrrolidine; DEHP, di(2-ethylhexyl)phthalate; AAP, acetaminophen.
[a]Data are mean ± SD values.
*$P < 0.01$ (vs. control).
**$P < 0.01$ (vs. IQ, NPYR, AAP, and control).

GST-P-positive liver cell foci (Figure 1B and D) corresponding to such altered foci were significantly ($P < 0.01$ and $P < 0.05$) increased in the IQ-treated and NPYR-treated groups in terms of number as well as area, but few were observed in the DEHP-treated, AAP-treated, and untreated control rats (Table 2). NPYR at a dose of 200 ppm was much more effective at inducing GST-P-positive foci than IQ at a dose of

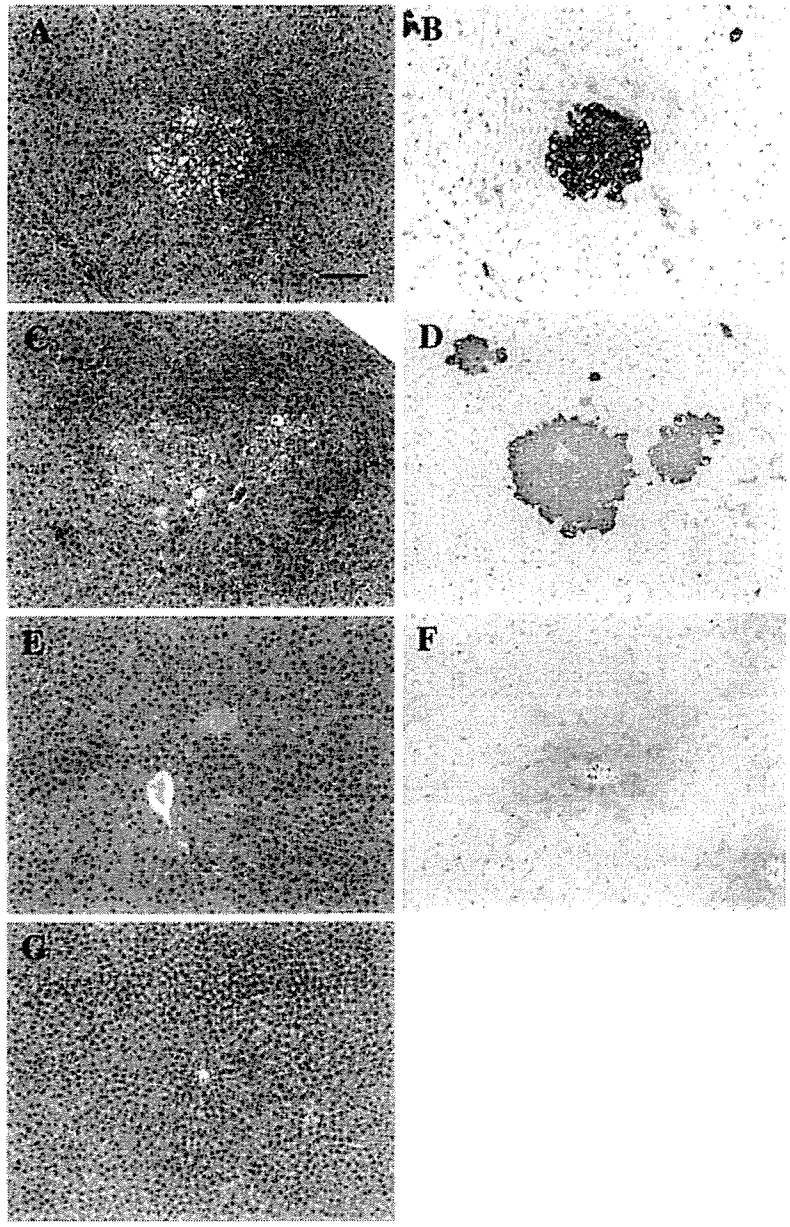

Figure 1. Histopathological findings (A, C, E, G) and immunohistochemistry for glutathione *S*-transferase placental form (GST-P) (B, D, F). Clear cell foci in the liver of rats given 2-amino-3-methylimidazo[4,5-*f*]quinoline (IQ) (A) and *N*-nitrosopyrrolidine (NPYR) (C). GST-P stainability corresponding to the foci A and C is evident (B and D). Marked centrilobular hypertrophy of liver cells is observed in a rat treated with di(2-ethylhexyl)phthalate (DEHP) (E). Faint and insignificant stainability of GST-P is found around the central veins of the liver of a rat treated with acetaminophen (AAP) (F). Appearance of the intact liver of a nontreated rat (G). Original magnification: ×180, Bar: 100 μm

Table 2. Numbers and Areas of GST-P Positive Liver Cell Foci

Treatment	Number of rats	Dose (ppm)	Number of foci/cm^2[a]	Area of foci (mm^2/cm^2)[a]
IQ	5	300	5.06 ± 1.52**	0.15 ± 0.06**
NPYR	5	200	24.05 ± 18.95*,***	1.09 ± 1.14*
DEHP	5	12 000	0.25 ± 0.17	<0.01
AAP	5	10 000	0.62 ± 0.44	<0.01
Control	5	—	0.48 ± 0.46	<0.01

[a]Data are mean ± SD values.
*$P < 0.05$ (vs. control).
**$P < 0.01$ (vs. control).
***$P < 0.05$ (vs. IQ).

300 ppm. Moreover, it was noteworthy that GST-P-positive single hepatocytes, which were not counted as the foci, were frequently observed in livers of the NPYR-treated rats. In the DEHP-treated rats, marked centrilobular hypertrophy of hepatocytes was observed throughout the whole liver (Figure 1E), although GST-P was consistently negative. In the AAP-treated rats, faint stainability for GST-P was detected in liver cells around the central veins, but these were not regarded as foci because of differences in staining intensity and diffuse location (Figure 1F).

Mutation Assays

Data for *gpt* MFs analyzed by 6-TG selection are summarized in Table 3. Identical mutations occurring in the same individual were omitted to avoid possible overlapping due to clonal proliferation. In the IQ-treated and NPYR-treated rats, *gpt* MFs in the liver DNA after clonal correction numbered 188.0×10^{-6} and 56.5×10^{-6}, approximately 35-fold and 10-fold higher, respectively, than the nontreatment control value (5.5×10^{-6}). There were no increases of *gpt* MFs in the liver DNA of the DEHP-treated (3.3×10^{-6}) and AAP-treated rats (5.5×10^{-6}) as compared to the nontreatment control value.

The *gpt* mutation spectra were analyzed by sequencing the *gpt* gene amplified from the mutants (Table 4). Because several mutants had two mutations in the *gpt* gene, the total number of mutations was larger than the number of mutants. In the IQ-treated rats, the predominant type of base substitution was the G:C to T:A transversion (62/109 = 56.9%), 45.2% (28/62) of which occurred at 5′-CpG-3′ sites. Most deletions occurred at G:C base pairs (9/10). In the NPYR-treated rats, the predominant type of base substitution was the A:T to G:C transition (33/67 = 49.3%) which was rare in the other groups. The numbers of G:C base substitutions were similar to the control levels. In the nontreatment control, DEHP-treated and AAP-treated rats, the most frequently observed mutation was the G:C to A:T transition. A:T to T:A transversions were observed in common in all the groups at a steady rate (18.2–34.8%). Most of them occurred at the same A:T base pair, the 299th in the *gpt* gene regardless of the experimental treatment.

Spi$^-$ selection for deletion mutations was performed for the DEHP-treated and nontreatment control cases. Spi$^-$ MFs were 4.5×10^{-6} and 4.3×10^{-6}, respectively (Table 5). Percentages of deletions larger than 1 kbp were 24.2 and 23.8 in the DEHP-treated and control rats, respectively. Thus, there were no differences in Spi$^-$ MF and deletion size spectrum between the DEHP-treated and control rats.

DISCUSSION

In order to understand the molecular mechanisms underlying chemical carcinogenesis in rats, *gpt* delta transgenic rats were here exposed to three established rodent hepatocarcinogens for 13-wk and

Table 3. Guanine Phosphoribosyltransferase (*gpt*) Mutant Frequencies (MFs) in the Liver

Treatment	Number of rats	Total population	Total *gpt* mutants	*gpt* mutants (clonal correction)	MF ($\times 10^{-6}$)[a]
IQ	5	525 000	133	89	188.0 ± 44.9*
NPYR	5	1 021 500	57	49	56.5 ± 24.5*,**
DEHP	5	3 247 500	9	9	3.3 ± 3.8
AAP	5	3 637 500	19	17	5.5 ± 5.6
Control	5	2 976 000	19	16	5.5 ± 2.4

[a]Data are mean ± SD values.
*$P < 0.01$ (vs. control).
**$P < 0.01$ (vs. IQ).

Table 4. Mutation Spectra of *gpt* Mutant Colonies

	Treatment				
Type	IQ	NPYR	DEHP	AAP	Control
Base substitution					
Transition					
G:C to A:T	6 (5.5)	5 (7.5)	5 (45.5)	9 (39.1)	8 (38.1)
A:T to G:C	1 (0.9)	33 (49.3)	0 (0)	0 (0)	0 (0)
Transversion					
G:C to T:A	62 (56.9)	3 (4.5)	3 (27.3)	5 (21.7)	2 (9.5)
G:C to C:G	1 (0.9)	0 (0)	0 (0)	0 (0)	0 (0)
A:T to T:A	26 (23.9)	20 (29.9)	2 (18.2)	8 (34.8)	7 (33.3)
A:T to C:G	1 (0.9)	3 (4.5)	0 (0)	0 (0)	0 (0)
Deletion	10 (9.2)	2 (3.0)	1 (9.1)	1 (4.3)	4 (19.0)
−1 bp	9	0	1	1	4
>2 bp	1	2	0	0	0
Insertion	0 (0)	0 (0)	0 (0)	0 (0)	0 (0)
Others	2 (1.8)	1 (1.5)	0 (0)	0 (0)	0 (0)
Total number of mutation	109 (100)	67 (100)	11 (100)	23 (100)	21 (100)

Numbers in parentheses are percentages.

in vivo mutation assays were performed. GST-P positive liver cell foci were significantly induced by IQ and NPYR, and marked hepatomegaly characterized by centrilobular hypertrophy of hepatocytes was observed in the DEHP-treated rats. Because these alterations are known as early intermediate endpoint lesions for rat hepatocarcinogenesis [32,33], the findings strongly suggest that the doses of these chemicals were sufficient to elicit carcinogenic responses in the livers of *gpt* delta rats in the present study. NPYR at a dose of 200 ppm induced more GST-P lesions than IQ at a dose of 300 ppm, indicating that NPYR is more carcinogenic in the present study, which is compatible with the previous carcinogenicity bioassays reporting 14/15 (93%) and 18/40 (45%) of tumor incidences with NPYR and IQ under the same condition, respectively [8,17]. However, MFs in the *gpt* target gene determined by 6-TG selection were three-times higher in the IQ-treated rats than in the NPYR-treated rats, indicating that the MF itself is not directly correlated with the carcinogenic activity of each compound. In the present mutagenicity assay, the MFs were determined from the mutation occurring in the reporter gene, which has no biological function. Carcinogenesis, however, should require the crucial mutations in the cancer-related genes for the initiation, and also promotional factors for the tumor development. Thus, it is not inconsistent that the carcinogenicity does not necessarily correlate with the in vivo mutagenicity simply in terms of intensity.

In vivo mutagenicity and mutation spectrum of IQ have been investigated in commercially available transgenic rodent models such as MutaMouse and BigBlue [20,34,35]. Because IQ is widely known to be a potent mutagen for the liver and induces mainly G:C to T:A transversion, it was used as an appropriate positive mutagen for validating the mutagenicity assay system. As expected, IQ proved positive, causing G:C to T:A transversions and deletions at G:C base pairs, confirming the reliability of *gpt* delta rats for in vivo mutagenicity assays. In view of the molecular mechanisms, two types of direct DNA adducts, the major *N*-(deoxyguanosin-8-yl)-IQ and the minor 5-(deoxyguanosin-N^2-yl)-IQ, are thought to be responsible for IQ-mutagenesis [19,36]. It has also been suggested that oxidative DNA damage with 8-OHdG formation as a result of nonenzymatic reduction of nitro-IQ may play a role in carcinogenesis [37]. Although, we could not determine which

Table 5. Spi^- MFs in the Liver

Treatment	Number of rats	Total population	Total Spi^- mutants	MF ($\times 10^{-6}$)[a]	Deletion size	
					<1 kb (%)	>1 kb (%)
DEHP	5	7 354 500	33	4.5 ± 2.5	25 (75.8)	8 (24.2)
Control	5	9 340 500	42	4.3 ± 2.5	32 (76.2)	10 (23.8)

[a]Data are mean ± SD values.

type of DNA lesion was responsible for the IQ-induced hepatocarcinogenesis, recent work with a panel of biomarkers for detecting oxidative stress, DNA damage, and expression of DNA repair enzymes in IQ-treated BigBlue rats pointed to specific DNA adducts rather than oxidative DNA damage as responsible for IQ initiation of hepatocarcinogenesis [38].

DEHP is categorized as a nongenotoxic carcinogen because it induces liver tumors in both sexes of rats and mice in a dose-dependent manner [21], with *Salmonella* in vitro mutagenicity assay being uniformly negative [22,23]. To the best of our knowledge, however, there is only one report testing in vivo mutagenicity of several nongenotoxic carcinogens, including DEHP, in *lacI* transgenic mice, which failed to detect mutagenicity [39]. In the present study, point mutations and deletion mutations were widely screened by 6-TG selection and Spi$^-$ selection, respectively, in order to analyze the possible involvement of genotoxicity caused by reactive metabolites or peroxisomal oxidative stress. However, no mutagenic activity of DEHP was detected in the liver of *gpt* delta rats after 13-wk of treatment. In the DEHP-treated rats, 27.3% of the total mutations were G:C to T:A transversions, known to be caused by 8-OHdG [40], while this was the case for 9.5% in the control rats. Because the *gpt* delta rat has relatively few copies of the transgene lambda EG10, the total number of mutants obtained was too small to allow accurate evaluation of the specific mutation spectrum, but the results do suggest that hepatocarcinogenesis by DEHP in rodents mainly depends on nongenotoxic or promotional mechanisms rather than direct DNA damage.

Despite extensive studies on the metabolism of NPYR or DNA modification by its metabolites, the in vivo mutation spectrum of NPYR in the mammalian species has not yet been determined. In the present study, NPYR predominantly induced A:T to G:C transitions in the liver of the *gpt* delta rats, accounting for 49.3% of all mutations in the *gpt* gene. This was unexpected because there have been a sufficient number of studies for providing specific adduct formations by NPYR with deoxyguanosine. NPYR is metabolically activated via alpha-hydroxylation by cytochrome P450 enzymes to yield reactive intermediates, 4-hydroxybutylaldehyde, and crotonaldehyde [41]. These metabolites can alkylate deoxyguanosine, and mainly result in exocyclic adducts such as N^7,C-8 guanine adducts and 1,N^2-propanodeoxyguanosine [42]. Because these adducts have also been found in DNA from tissues of NPYR- or crotonaldehyde-treated animals, they might be expected to be the major adducts formed in vivo [43,44]. NPYR-induced mutational spectra have been investigated in bacterial systems with the *lacI* gene and M13mp2 phage DNA as targets [12,13] and base substitutions at G:C base pairs appeared to predominate. In the present study, however, the predominant type of base substitution in the liver of NPYR-treated rats was evidently A:T to G:C, followed by A:T to T:A. The difference between in vitro and in vivo mutagenesis by NPYR may be partly explained by means of specific etheno-adduct formation due to reactions of crotonaldehyde with deoxyadenosine as well as deoxyguanosine, known to yield 1,N^6-ethenoadenosine [45]. This latter adduct is formed during lipid peroxidation [46], and has also been detected in tissues from rats treated with vinyl chloride, a hepatocarcinogen in humans and rodents [47]. In the present study, the livers of NPYR-treated rats contained a number of GST-P positive single liver cells which may be indicative of lipid peroxidation and its end products, unsaturated aldehydes such as 4-hydroxynonenal, acrolein, and crotonaldehyde [48]. 1,N^6-Ethenoadenosine has shown to be highly mutagenic in mammalian cells such as simian kidney cells, exclusively inducing A:T to G:C base substitutions, while the mutation efficiency in *E. coli* is relatively low [49]. Moreover, Barbin et al. have suggested that concomitant formation of the etheno-adducts may play a role in the hepatocarcinogenesis by vinyl chloride, due to A:T base mutation occurring in the *p53* tumor suppressor gene [50]. In addition to a possible metabolite, crotonaldehyde, from NPYR, these data thus provide a possible mutational mechanism mediated by lipid peroxidation, interpreting our present findings in NPYR-treated rats. For understanding the molecular mechanism of NPYR-induced hepatocarcinogenesis, the levels of mutagenic adenine or thymine adducts and the possible specific mutations in the cancer-related genes need to be further analyzed in the liver of NPYR-treated rats.

In conclusion, based on the characteristic mutation spectra here observed in IQ-treated and NPYR-treated *gpt* delta transgenic rats, the predominant occurrence of A:T to G:C transitions in the NPYR-case suggests a possible contribution of the minor adenine adduct 1,N^6-ethenoadenosine to its in vivo mutagenesis in mammals, even though this carcinogen has been reported to form mainly guanine adducts in vitro. No mutagenic activity was detected in DEHP-treated rats, supporting the promotion pathway of DEHP-induced hepatocarcinogenesis rather than direct DNA damage. Our data also indicate that analysis of the specific in vivo mutational spectrum can provide crucial information for understanding the molecular mechanisms underlying chemical carcinogenesis.

ACKNOWLEDGMENTS

We thank all individuals of Division of Genetics and Mutagenesis, National Institute of Health Sciences for technical advices and valuable suggestions for the mutation assays. This work was supported in part by a grant for Research Fellow of the Japan Society for the Promotion of Science, a

Grant-in-aid (12-9) for Cancer Research from the Ministry of Health, Labor, and Welfare of Japan, and a Grant-in-aid (13670235) for Scientific Research from the Ministry of Education, Culture, Sports, Science, and Technology of Japan.

REFERENCES

1. Lijinsky W. Carcinogenicity and mutagenicity of *N*-nitroso compounds. Mol Toxicol 1987;1:107–119.
2. Tennant RW, Elwell MR, Spalding JW, Griesemer RA. Evidence that toxic injury is not always associated with induction of chemical carcinogenesis. Mol Carcinog 1991;4: 420–440.
3. Crebelli R, Conti L, Fuselli S, Leopardi P, Zijno A, Carere A. Further studies on the comutagenic activity of cigarette smoke condensate. Mutat Res 1991;259:29–36.
4. Godard T, Fessard V, Huet S, et al. Comparative in vitro and in vivo assessment of genotoxic effects of etoposide and chlorothalonil by the comet assay. Mutat Res 1999;444: 103–116.
5. Nohmi T, Suzuki T, Masumura K. Recent advances in the protocols of transgenic mouse mutation assays. Mutat Res 2000;455:191–215.
6. Hayashi H, Kondo H, Masumura K, Shindo Y, Nohmi T. Novel transgenic rat for in vivo genotoxicity assays using 6-thioguanine and Spi$^-$ selection. Environ Mol Mutagen 2003;41:253–259.
7. Nohmi T, Katoh M, Suzuki H, et al. A new transgenic mouse mutagenesis test system using Spi$^-$ and 6-thioguanine selections. Environ Mol Mutagen 1996;28:465–470.
8. Lijinsky W, Taylor HW. The effect of substituents on the carcinogenicity of *N*-nitrosopyrrolidine in Sprague-Dawley Rats. Cancer Res 1976;36:1988–1990.
9. Bartsch H, O'Neill IK, Castegnaro M, Okada M. Evaluation of the carcinogenic risk of chemicals to humans: Some *N*-nitroso compounds. IARC Sci Publ 1978;39:313–326.
10. Wang M, MacIntee EJ, Shi Y, et al. Reactions of alpha-acetoxy-*N*-nitrosopyrrolidine with deoxyguanosine and DNA. Chem Res Toxicol 2001;14:1435–1445.
11. Guttenplan JB. *N*-nitrosamines: Bacterial mutagenesis and in vitro metabolism. Mutat Res 1987;186:81–134.
12. Ziellenska M, Ahmed A, Glickman BW. Mutational specificities of environmental carcinogens in the *lacI* gene of *Escherichia coli*. III: The cyclic nitrosamine *N*-nitrosopyrrolidine is a complex mutagen. Mol Carcinog 1990;3:122–125.
13. Arimoto KS, Anma N, Yoshinaga Y, Douki T, Cadet J, Hayatsu H. Oxidative damage and induced mutations in m13mp2 phage DNA exposed to *N*-nitrosopyrrolidine with UVA radiation. Mutagenesis 2000;15:473–477.
14. IARC. IQ (2-amino-3-methylimidazo[4,5-*f*]quinoline). In: Some naturally occurring substances: Food items and constituents, heterocyclic aromatic amines and mycotoxins. IARC monograph on the evaluation of carcinogenic risk of chemicals to humans. 1993;56:165–195.
15. Griciute L. Carcinogenicity of *N*-nitroso compounds and their possible role in the development of human cancer. IARC Sci Publ 1978;18:3–9.
16. Yamashita M, Wakabayashi K, Nagao M, et al. Detection of 2-amino-3-methylimidazo[4,5-*f*]quinoline in cigarette smoke condensate. Jpn J Cancer Res (Gann) 1986;77:419–422.
17. Ohgaki H, Hasegawa H, Kato T, et al. Carcinogenicity in mice and rats of heterocyclic amines in cooked foods. Environ Health Perspect 1986;67:129–134.
18. Adamson RH, Thorgeirsson UP, Snyderwine EG, et al. Carcinogenicity of 2-amino-3-methylimidazo[4,5-*f*]quinoline in non-human primates: Induction of tumors in three macaques. Jpn J Cancer Res 1990;81:10–14.
19. Schut HAJ, Snyderwine EG. DNA adducts of heterocyclic amine food mutagens: Implications for mutagenesis and carcinogenesis. Carcinogenesis 1999;20:353–368.
20. Bol SA, Horlbeck J, Markovic J, de Boer JG, Turesky RJ, Constable A. Mutational analysis of the liver, colon, and kidney of BigBlue rats treated with 2-amino-3-methylimidazo[4,5-*f*]quinoline. Carcinogenesis 2000;21:1–6.
21. Kluwe WM, McConnell EE, Huff JE, Haseman JK, Douglas JF, Hartwell WV. Carcinogenicity testing of phthalate esters and related compounds by the National Toxicology Program and the National Cancer Institute. Environ Health Perspect 1982; 45:129–133.
22. Kirby PE, Pizzarello RF, Lawlor TE, Haworth SR, Hodgson JR. Evaluation of di-(2-ethylhexyl)phthalate and its major metabolites in the Ames test and L5178Y mouse lymphoma mutagenicity assay. Environ Mutagen 1983;5: 657–663.
23. Zeiger E, Haworth S, Mortelmans K, Speck W. Mutagenicity testing of di(2-ethylhexyl)phthalate and related chemicals in *Salmonella*. Environ Mutagen 1985;7:213–232.
24. Yagi YK, Shimoi N. Teratogenicity and mutagenicity of a phthalate ester. Teratology 1976;14:259–260.
25. Tomita I, Nakamura Y, Aoki N, Inui N. Mutagenic/carcinogenic potential of DEHP and MEHP. Environ Health Perspect 1982;45:119–125.
26. Takagi A, Sai K, Umemura T, Hasegawa R, Kurokawa Y. Significant increase of 8-hydroxydeoxyguanosine in liver DNA of rats following short-term exposure to the peroxisome proliferators di-(2-ethylhexyl)phthalate and di-(2-ethylhexyl)adipate. Jpn J Cancer Res 1990;81:213–215.
27. Seo KW, Kim KB, Kim YJ, Choi JY, Lee KT, Choi KS. Comparison of oxidative stress and changes of xonobiotic metabolizing enzymes induced by phthalates in rats. Food Chem Toxicol 2004;42:107–114.
28. Gorelick NJ. Overview of mutation assays in transgenic mice for routine testing. Environ Mol Mutagen 1995;25: 218–230.
29. Mirsalis JC, Monforte JA, Wineger RA. Transgenic animal models for detection of in vivo mutations. Ann Rev Pharmacol Toxicol 1995;35:145–164.
30. de Boer JG. Protection by dietary compounds against mutation in a transgenic rodent. J Nutr 2001;131:3082S–3086S.
31. Nishikawa A, Suzuki T, Masumura K, et al. Reporter gene transgenic mice as a tool for analyzing the molecular mechanisms underlying experimental carcinogenesis. J Exp Clin Cancer Res 2001;20:111–115.
32. Ito N, Hasegawa R, Imaida K, et al. Medium-term rat liver bioassay for rapid detection of hepatocarcinogenic substances. J Toxicol Pathol 1997;10:1–11.
33. Takagi A, Sai K, Umemura T, Hasegawa R, Kurokawa Y. Hepatomegaly is an early biomarker for hepatocarcinogenesis induced by peroxisome proliferators. J Environ Pathol Toxicol Oncol 1992;11:145–149.
34. Ushijima T, Hosoya Y, Ochiai M, et al. Tissue-specific mutational spectra of 2-amino-3,4-dimethylimidazo[4,5-*f*]quinoline in the liver and bone marrow of *lacI* transgenic mice. Carcinogenesis 1994;15:2805–2809.
35. Davis CD, Dacquel HAJ, Schut SS, Thorgeirsson SS, Snyderwine EG. In vivo mutagenicity and DNA adduct levels of heterocyclic amines in Muta^{TM}Mice and *c-myc/lacZ* double transgenic mice. Mutat Res 1996;356:287–296.
36. Turesky RJ, Gremaud E, Markovic J, Snyderwine EG. DNA adduct formation of the food-derived mutagen 2-amino-3,4-dimethylimidazo[4,5-*f*]quinoline in nonhuman primates undergoing carcinogen bioassay. Chem Res Toxicol 1996;9: 403–408.
37. Murata M, Kobayashi M, Kawanishi S. Nonenzymatic reduction of nitro derivative of a heterocyclic amine IQ by NADH and Cu(II) leads to oxidative DNA damage. Biochemistry 1999;38:7624–7629.

38. Moller P, Wallin H, Vogel U, et al. Mutagenicity of 2-amino-3-methylimidazo[4,5-*f*]quinoline in colon and liver of BigBlue rats: Role of DNA adducts, strand breaks, DNA repair, and oxidative stress. Carcinogenesis 2002;23:1379–1385.
39. Gunz D, Shephard SE, Lutz WK. Can nongenotoxic carcinogens be detected with the *lacI* transgenic mouse mutation assay? Environ Mol Mutagen 1993;21:209–211.
40. Moriya M. Single-stranded shuttle phagemid for mutagenesis studies in mammalian cells: 8-oxoguanine in DNA induces targeted G:C-T:A transversions in simian kidney cells. Proc Natl Acad Sci USA 1993;90:1122–1126.
41. Wang M, Chung FL, Hecht SS. Identification of crotonaldehyde as a hepatic microsomal metabolite formed by alpha-hydroxylation of the carcinogen *N*-nitrosopyrrolidine. Chem Res Toxicol 1988;1:28–31.
42. Wang M, Chung FL, Hecht SS. Formation of acyclic and cyclic guanine adducts in DNA reacted with α-acetoxy-*N*-nitrosopyrrolidine. Chem Res Toxicol 1989;2:423–428.
43. Hunt EJ, Shank RC. Formation and persistence of a DNA adduct in rodents treated with *N*-nitrosopyrrolidine. Carcinogenesis 1991;12:571–575.
44. Chung FL, Young R, Hecht SS. Detection of cyclic 1,N^2-propanodeoxyguanosine adducts in DNA of rats treated with *N*-nitrosopyrrolidine and mice treated with crotonaldehyde. Carcinogenesis 1989;10:1291–1297.
45. Chen HJ, Chung FL. Formation of etheno adducts in reactions of enals via autoxidation. Chem Res Toxicol 1994; 7:857–860.
46. el Ghissassi F, Barbin A, Nair J, Bartsch H. Formation of 1,N^6-ethenoadenine and 3,N^4-ethenocytosine by lipid peroxidation products and nucleic acid bases. Chem Res Toxicol 1995; 8:278–283.
47. Guichard Y, el Ghissassi F, Nair J, Bartsch H, Barbin A. Formation and accumulation of DNA ethenobases in adult Sprague-Dawley rats exposed to vinyl chloride. Carcinogenesis 1996;17:1553–1559.
48. Satoh K, Hayakari M, Ookawa K, et al. Lipid peroxidation end products-responded induction of a preneoplastic marker enzyme glutathione *S*-transferase P-form (GST-P) in rat liver on administration via the portal vein. Mutat Res 2001;483: 65–72.
49. Pandya GA, Moriya M. 1,N^6-ethenodeoxyadenosine, a DNA adduct highly mutagenic in mammalian cells. Biochemistry 1996;35:11487–11492.
50. Barbin A, Froment O, Boibin S, et al. *p53* Gene mutation pattern in rat liver tumor induced by vinyl chloride. Cancer Res 1997;57:1695–1698.